Original Article

Albumin-induced premature senescence in human renal proximal tubular cells and its relationship with intercellular fibrosis

Wen Lu, Shijing Ren, Wenhui Dong, Xiaomin Li, Zongji Zheng, Yijie Jia, and Yaoming Xue*

Department of Endocrinology and Metabolism, Nanfang Hospital, Southern Medical University, Guangzhou 510000, China
*Correspondence address. Tel: +86-20-61641637; E-mail: xueyaoming999@126.com

Abstract

The presence of senescent cells is associated with renal fibrosis. This study aims to investigate the effect of albumin-induced premature senescence on tubulointerstitial fibrosis and its possible mechanism *in vitro*. Different concentrations of bovine serum albumim (BSA) with or without si-p21 are used to stimulate HK-2 cells for 72 h, and SA-β-gal activity, senescence-associated secretory phenotypes (SASPs), LaminB1 are used as markers of senescence. Immunofluorescence staining is performed to characterize the G2/M phase arrest between the control and BSA groups. Alterations in the DNA damage marker γ-H2AX, fibrogenesis, and associated proteins at the G2/M phase, such as p21, p-CDC25C and p-CDK1, are evaluated. Compared with those in the control group, the SA-β-gal activity, SASP, and γ-H2AX levels are increased in the BSA group, while the level of LaminB1 is decreased. Meanwhile, HK-2 cells blocked at the G2/M phase are significantly increased under the stimulation of BSA, and the levels of p21, p-CDC25C and p-CDK1, as well as fibrogenesis are also increased. When p21 expression is inhibited, the levels of p-CDC25C and p-CDK1 are decreased and the G2/M phase arrest is improved, which decreases the production of fibrogenesis. In conclusion, BSA induces renal tubular epithelial cell premature senescence, which regulates the G2/M phase through the CDC25C/CDK1 pathway, leading to tubulointerstitial fibrosis.

Key words senescence, human renal proximal tubular cell, fibrosis, G2/M arrest, p21, albuminuria

Introduction

In the past few decades, the global prevalence of diabetes mellitus (DM) has increased significantly. Therefore, the global prevalence of DM-related microvascular and macrovascular complications is increasing dramatically [1]. Diabetic kidney disease (DKD) is the major complication leading to end-stage renal disease (ESRD). The incidence of DKD has increased by more than folds in the past decade, and it accounts for approximately 50% of all ESRDs worldwide. The primary feature of DKD is albuminuria, which can be detected in its earliest stage. Without intervention, micro-albuminuria may progress to severe albuminuria in approximately 50% of patients, and the risk of progression to ESRD is 10 times higher in albuminuria patients than in patients without albuminuria [2,3]. Renal fibrosis is an inevitable outcome of all progressive chronic renal diseases [4], and albuminuria promotes renal interstitial inflammation and fibrosis [5,6]. Previous studies showed that renal protection can be achieved by reducing albuminuria [7].

Therefore, exploring the internal mechanisms of renal injury caused by albuminuria are of great significance to prevent the progression of renal fibrosis and protect renal function.

In recent years, studies have revealed the important role of renal tubular epithelial cells (TECs) in renal fibrosis [8]. There is evidence that TECs may be the initiator of renal fibrosis [9]. Different methods can be used to repair the renal injury under different pathological conditions. If the injury is mild and transient, the renal function can be restored to normal [10,11]. However, if the injury is severe and persistent, TECs may lead to maladaptive repair, thereby exacerbating renal fibrosis [10,12]. A maladaptive repair is characterized by interstitial fibrosis, renal tubule atrophy and sparse capillaries [12]. Therefore, keeping or improving the functional status of TECs plays an important role in protecting the kidneys and in delaying fibrosis.

Renal TECs without an adaptive repair show cellular senescence, and cellular senescence is involved in the development of many

diseases, such as cardiovascular, liver, and kidney diseases [13]. Therefore, preventing cellular senescence may be an important approach to inhibit the development of kidney diseases [14]. Therefore,and the emerging role of cellular senescence in DKD has attracted much attention [15], but still lack of comprehensive and systematic study. One of the most important features of cellular senescence is cell cycle arrest [10–12]. Previous studies suggested that TECs arrested at the G2/M phase after injury promote renal fibrosis [16]. The cyclin-dependent kinase (CDK) inhibitor p21, which is widely recognized as a key regulator of cell cycle checkpoints [17], could induce cellular G2/M arrest [18] and serve as a marker of cellular senescence [19]. Kitada *et al.* [20] constructed an animal DKD model and found that the SA-β-gal activity and p21 expression increased in the renal cortex. Moreover, they localized p21-positive cells in renal tissues and found p21 staining in the proximal tubule of the renal cortical region, suggesting the presence of cellular senescence in the tubules in the course of DKD, which may be related to p21 [20]. However, whether renal TEC senescence-induced DKD is associated with an increased albuminuria and whether cellular senescence is the cause of albuminuria-induced tubulointerstitial fibrosis are still unclear.

Therefore, in this study we explored whether albuminuria can induce premature senescence *in vitro* and its possible molecular mechanism that contributes to renal TEC fibrosis. Our results showed that albuminuria induces premature senescence in HK-2 cells. The expression of p21 is increased in senescent renal TECs, and p21 leads to cells arrested at the G2/M phase through the CDC25C/CDK1 pathway, which results in the production of fibrogenic factors. Therefore, regulating the cell cycle by p21 to delay the premature senescence may be a possible new way to improve renal tubulointerstitial fibrosis in DKD.

Materials and Methods
Cell culture and transfection
Human proximal tubule cell line (HK-2) was obtained from ATCC (Rockville, USA). The cells were grown in a Dulbecco's modified Eagle medium (DMEM) containing 5.5 mM glucose and 10% fetal bovine serum (FBS). Before the intervention, the cell growth cycle was synchronized by starvation treatment with DMEM containing 2% FBS for 72 h. Bovine serum albumin (BSA; Sigma-Aldrich, St Louis, USA) was used to stimulate HK-2 cells to mimic DKD *in vitro.* Then, 50 nM si-p21 (5′-AGACCATGTGGACCTGTCA-3′; RiboBio, Guangzhou, China) was used to knockdown p21 in HK-2 cells. All transfections were conducted using Lipofectamine® 3000 (Invitrogen, Carlsbad, USA) according to the manufacturer's instructions.

Senescence-associated β-galactosidase staining
HK-2 cells were seeded in 6-well plates with BSA (0–20 mg/mL) for 72 h. Senescence-associated β-galactosidase (SA-β-gal) staining was performed using a senescence β-galactosidase staining kit (Beyotime, Shanghai, China) according to the manufacturer's instructions. After the treatment, the cells were washed twice with PBS and fixed with a fixative solution for 15 min at room temperature. Then, the cells in each well were stained with 1 mL of complete β-gal staining solution overnight at 37°C. Cell images were captured using an IX73 microscope (Olympus, Tokyo, Japan).

Quantitative real-time polymerase chain reaction
Total RNA was isolated from HK-2 cells using a Trizol reagent

(TaKaRa, Dalian, China) according to the manufacturer's protocols. The RNA concentration and purity were detected with a NanoDrop ND-1000 spectrophotometer (Thermo Fisher Scientific, Wilmington, USA). Reverse transcription was performed using Prime-Script™ RT Master Mix (TaKaRa). Quantitative real-time polymerase chain reaction (qRT-PCR) was conducted on a Roche Light Cycler 480 Real-time PCR System (Roche, Basel, Switzerland) using SYBR® Premix Ex Taq™ (TaKaRa). The primer sequences are listed in Table 1. The expression of each gene was calculated using the $2^{-\Delta\Delta Ct}$ method, and *18S* was used as an internal control.

Immunofluorescence staining
HK-2 cells were plated in 12-well plates with 20 mg/mL BSA for 72 h. After 72 h of treatment with BSA or si-p21 transfection, the cells were fixed with an immunol staining fix solution (Beyotime) for 15 min and blocked with an immunol staining blocking buffer (Beyotime) for 30 min. Then, after being rinsed with PBS for three times (5 min each), the cells were incubated with primary antibodies against p-PH3Ser10 (1:500; Cell Signaling Technology, Beverly, USA) and LaminB1 (1:50; Cell Signaling Technology) at 4°C overnight. After three times wash with PBS, the cells were incubated with FITC-conjugated goat anti-rabbit IgG (1:100; ProteinTech, Rosemont, USA) or FITC-conjugated goat anti-mouse IgG (1:100; ProteinTech) secondary antibody in the dark for 1 h. Finally, the nuclei were counterstained with DAPI. The slides were visualized for immunofluorescence and FISH with a fluorescence microscope at a magnification of ×400. The images were analyzed using ImageJ software.

Western blot analysis
The total protein was extracted from cells using a cold RIPA lysis buffer. Protein samples (20 μg) were separated by 12.5% sodium dodecyl sulfate polyacrylamide gel electrophoresis and transferred to polyvinylidene difluoride membranes (Millipore, Billerica, USA). The membranes were blocked in a QuickBlock™ blocking buffer (Beyotime) for 30 min and then incubated with primary antibodies including anti-p21 (1:800; ProteinTech), anti-α-SMA (1:1000; ProteinTech), anti-CTGF (1:800; Sangon Biotech, Shanghai, China), anti-CDK1(Tyr15) (1:1000; Cell Signaling Technology), anti-CDC25C(Ser216) (1:1000; Cell Signaling Technology), and anti-GAPDH (1:5000; ProteinTech) at 4°C overnight. Subsequently, the membranes were incubated with the corresponding HRP-conjugated secondary antibodies at room temperature for 1 h. Finally, protein bands were visualized using a chemiluminescence kit

Table 1. Sequence of the primers used for qRT-PCR

Gene	Primer sequence (5′→3′)	
IL-1α	Forward	TGGTAGTAGCAACCAACGGGA
	Reverse	ACTTTGATTGAGGGCGTCATTC
IL-6	Forward	CAATAACCACCCCTGACC
	Reverse	GCGCCAGAATGAGATGAGTT
IL-8	Forward	TTTTGCCAAGGAGTGCTAAAGA
	Reverse	AACCCTCTGCACCCAGTTTTC
p21	Forward	TGTCCGTCAGAACCCATGC
	Reverse	AAAGTCGAAGTTCCATCGCTC
18S	Forward	AACCCGTTGAACCCCATT
	Reverse	CCATCCAATCGGTAGTAGCG

(Fdbio Science, Hangzhou, China), and the images were analyzed using ImageJ software. GAPDH was used as the loading control.

Statistical analysis

Results were analyzed using the SPSS 25.0 software. Data are presented as the mean ± SEM. One-way ANOVA or Kruskal-Wallis H test was used to determine the statistical significance according to the results of the normal distribution test. $P < 0.05$ was considered statistically significant.

Results

BSA induced changes in senescent phenotypes

Proximal tubule cells exhibit a senescent phenotype very early in response to diabetes. Targeting these senescent-like cells could potentially attenuate diabetic complications [21]. The senescence of renal TECs (HK-2) induced by BSA was evaluated *in vitro*. First, the morphology of HK-2 cells treated with 0–20 mg/mL BSA for 72 h was analyzed (Figure 1A). As the concentration of BSA increased, the cell morphology became more irregular compared with the control group. In addition, the cell density in the BSA group decreased significantly at high BSA concentration (20 mg/mL), in-

dicating that cell proliferation was inhibited. To further confirm this result, a classical senescence assay (SA-β-Gal staining) was performed (Figure 1B). Compared with the control group, BSA induced a higher level of SA-β-gal activity, which was proportional to the BSA concentration. It is known that senescence-associated secretory phenotypes (SASPs) play an important role in the pathophysiological activity of senescent cells [19]; therefore, IL-1α, IL-6 and IL-8, which are the common SASP components, were investigated by qRT-PCR [19]. Results showed that 72 h of treatment with 20 mg/mL BSA significantly promoted the expressions of IL-1α, IL-8, and IL-6, indicating that BSA induced the expression of SASPs in HK-2 cells (Figure 1C–E). These results verified that BSA indeed caused a senescent phenotype.

BSA downregulated LaminB1 and stimulated the expression of γ-H2AX

A common mark of senescent cells is the loss of LaminB1, a structural protein in the nuclear lamina [22,23]. To evaluate the effect of BSA on the nuclear membrane integrity of HK-2 cells, immuno-fluorescence microscopy was used to detect the expression and location of LaminB1 in HK-2 cells. The results showed that the
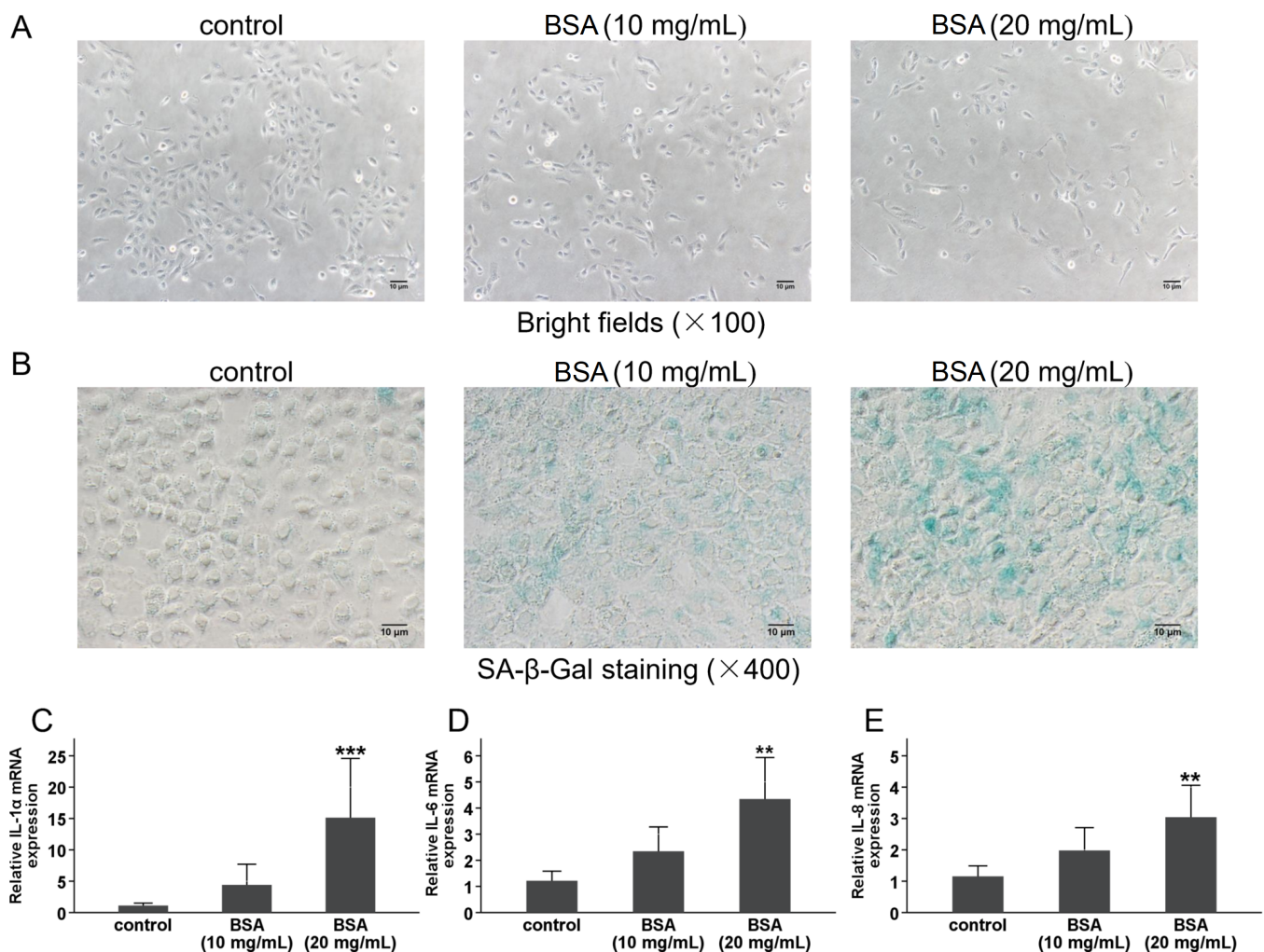
Figure 1. BSA induced changes in senescent phenotypes (A) HK-2 cells morphology varied in response to 0–20 mg/mL BSA for 72 h. (B) SA-β-gal staining showed a dose-dependent increase of SA-β-gal activity after treatment with BSA for 72 h in HK-2 cells. (C–E) The expressions of the SASP factors IL-1α, IL-6 and IL-8 were detected by qRT-PCR after treatment with BSA or with normal medium as control for 72 h in HK-2 cells. **$P < 0.01$, and ***$P < 0.001$ vs control.

expression of LaminB1 (green) on the nuclear membrane of HK-2 cells was significantly reduced after the treatment with 20 mg/mL BSA for 72 h, compared with that in the control (Figure 2A,B). Meanwhile, transcriptomic studies demonstrated that the down-regulation of LaminB1 mRNA is a widespread marker of senescence [22]. Therefore, the expression of LaminB1 mRNA was detected by qRT-PCR. When HK-2 cells were treated with 20 mg/mL BSA for 72 h, the expression of LaminB1 mRNA was decreased by 43% compared with that in the control cells (Figure 2C). Subsequently, to investigate whether BSA induces DNA damage, the expression of the DNA double-strand break marker γ-H2AX, which is also a senescence marker [24], was analyzed. Compared with the control cells, HK-2 cells treated with 20 mg/mL BSA for 72 h showed an increased γ-H2AX expression (1.5 folds; Figure 2D,E). The decrease in LaminB1 and increase in γ-H2AX further suggested that BSA could induce the senescence of HK-2 cells.

BSA induced the G2/M phase arrest and p21 expression

Previous studies showed that chronic kidney disease is associated with insufficient cell cycle progression of renal TECs, which stay in G2/M stages [16,25–27]. We probed whether the aging process induced by BSA in HK-2 cells could contribute to the G2/M arrest by using specific immunofluorescence antibodies for the phosphorylation of histone H3 at Ser10(p-H3), which represents only the cells at the G2/M phase [16]. It was found that p-H3 (+) cells were increased gradually with the increase in BSA concentration (Figure 3A). The percentage of p-H3 (+) cells treated with 20 mg/mL BSA for 72 h was 28-fold higher compared to that in the control group (Figure 3B). p21 is a known inducer of cellular G2/M arrest [28]. Therefore, the cell cycle-dependent protein kinase inhibitor p21 expression was analyzed. HK-2 cells were treated with BSA for 72 h, and the expression of p21 was detected by qRT-PCR and western blot analysis. Compared with that in the control cells, the mRNA level of p21 was increased by 3.2 times in cells treated with 20 mg/mL BSA (Figure 3C), while the p21 protein level was increased by 59% (Figure 3D,E). Our data showed that BSA may induce p21 upregulation to cause HK-2 cell arrest at the G2/M phase.

BSA stimulated the profibrotic factors in HK-2 cells

Previous studies showed that renal TECs in G2/M phase arrest generate more profibrotic factors [16]. To investigate whether albuminuria is involved in fibrosis, HK-2 cells were treated with different concentrations of BSA to observe the changes in fibrosis *in vitro*. Western blot analysis also revealed that the expressions of CTGF and α-SMA were increased in the 20 mg/mL BSA-treated group compared with that in the control group (Figure 4). CTGF was increased by 48% after stimulation with 20 mg/mL BSA (Figure 4A, B), and the α-SMA level in the 20 mg/mL BSA-treated group was 3.9 times as high as that in the control group (Figure 4A,C). These data showed that BSA can induce fibrosis in HK-2 cells.

Inhibition of p21 prevented the G2/M arrest and fibrogenesis in HK-2 cells

As a member of the cyclin-dependent kinase inhibitor (CDKI) family, p21 is a well-known important cytokine that can induce cellular G2/M arrest [18,28]. We explored whether BSA stimulates the expression of p21 in HK-2 cells, which leads to G2/M phase arrest and promotes the production of fibrosis factors. Changes in cell cycle and fibrogenic factors were detected after downregulating the

p21 expression. The expression of p21 protein was decreased after the transfection with si-p21 in 20 mg/mL BSA-treated HK-2 cells (Figure 5A,B). Subsequently, compared with the BSA-treated group, transfection with si-p21 combined with BSA treatment significantly improved the G2/M phase arrest of HK-2 cells, as observed by immunofluorescence microscopy (Figure 5C,D). Furthermore, western blot analysis showed that after the knockdown of p21 by si-p21 transfection in the BSA-treated group, the expressions of CTGF and α-SMA were significantly reduced compared with those in the BSA alone group (Figure 5E–H). The results showed that BSA induced the G2/M phase arrest, leading to an increase in intracellular profibrotic factors in HK-2 cells, which might be related to the increased p21 expression.

### BSA caused the G2/M phase arrest by activating the CDC25C/CDK1 pathway

To explore the molecular mechanisms of the G2/M phase arrest induced by p21, intracellular signaling was studied. The increased phosphorylation of CDC25C and CDK1 is the hallmark of cell cycle arrest at the G2/M phase [29]. The results showed that as the BSA concentration increased, the phosphorylation of CDC25C and CDK1 was also increased (Figure 6A–D). Then, si-p21 was used to transfect HK-2 cells treated with 20 mg/mL BSA, which decreased the phosphorylation level of CDK1 and CDC25C compared with that in the BSA alone group (Figure 6E–G). Thus, p21 may contribute to BSA-induced G2/M arrest by promoting the phosphorylation of CDC25C and CDK1.

Discussion

The morbidity and mortality of patients with DKD have been increasing rapidly worldwide [30–32]. Albuminuria is the primary feature of DKD, and it is positively correlated with the progression to ESRD [33]. It was reported that the exposure of proximal TECs to albumin causes tubulointerstitial fibrosis and promotes the progression of DKD [34–38]. Furthermore, in the early stage of DKD, the onset of albuminuria could affect the tubular function and induce morphological injury [39]. Thus, renal tubular cells play a key role in albuminuria-induced renal injury, and it is important to study the impact of albuminuria on renal tubular cell injury and its underlying mechanisms.

It was reported that cellular senescence plays a vital role in aging and diseased kidneys, and the clearance or depletion of senescent cells can relieve age-related damage and dysfunction in the kidneys [40]. In diabetic kidneys, accelerated senescent phenotypes are mainly found in tubular cells and podocytes [41]. Therefore, we hypothesize that the damage to renal TECs caused by albuminuria may be related to cellular senescence. Although it is unclear whether albumin can specifically induce renal TEC senescence, the effect of inhibiting the albumin uptake on renal TECs can still be found from previous studies. The reabsorption of albumin in renal TECs is mediated by endocytosis through Megalin and Cubilin receptors, so the reabsorption of albumin can be inhibited by inhibiting these receptors [42]. Liu *et al.* [43] found that inhibiting Megalin and/or Cubilin receptors to reduce the albumin uptake can block inflammatory cell activation and cytokine maturation. In a mouse model of nonselective proteinuria [44], albumin staining in renal TECs was significantly reduced after the specific deletion of Megalin receptors. At the same time, oxidative stress markers, inflammatory markers, and cell apoptosis were significantly improved
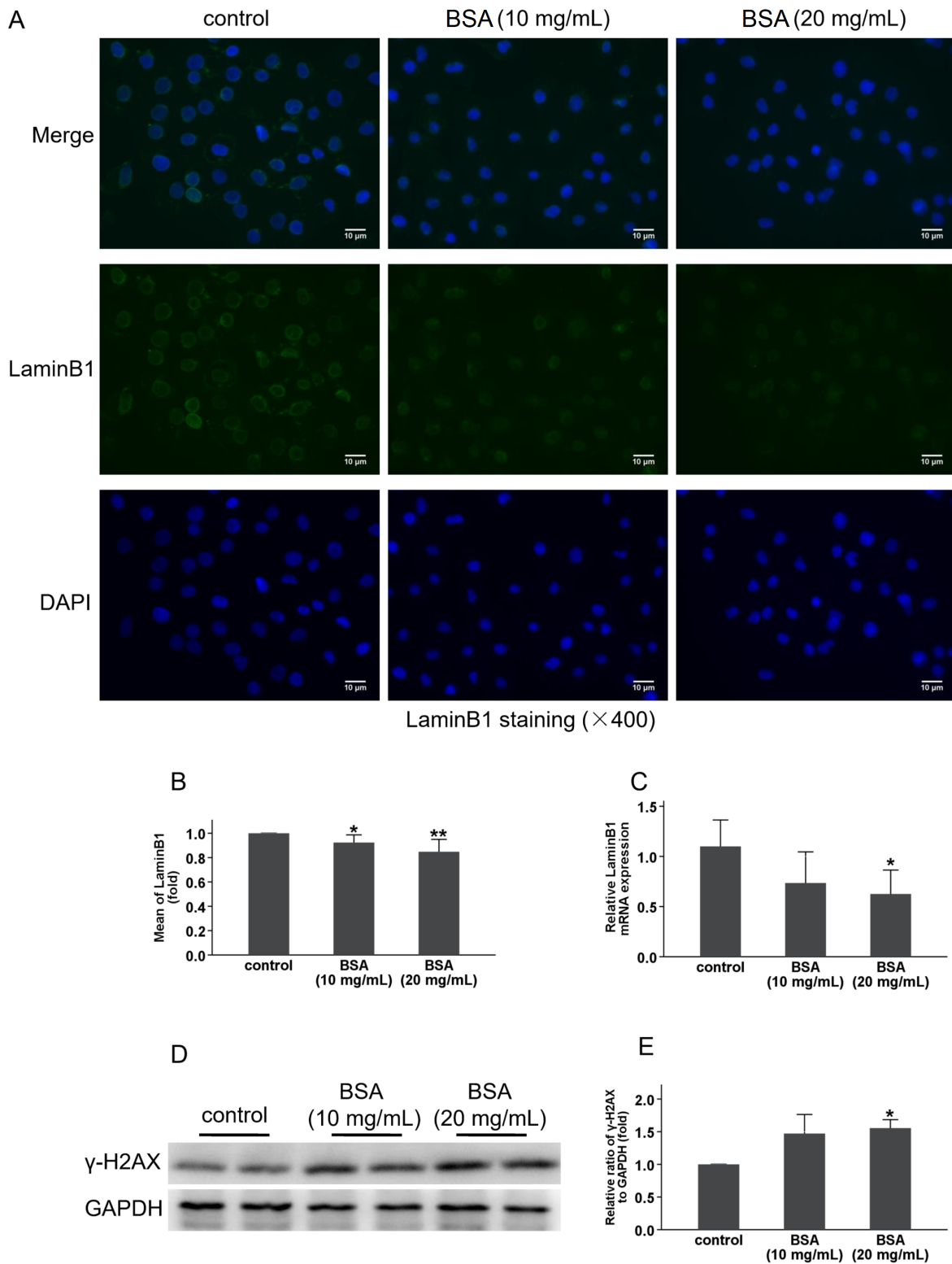
Figure 2. BSA downregulated LaminB1 and induced DNA damage (A) Immunofluorescence staining showed a concentration-dependent reduction of LaminB1 after treatment with BSA or with normal medium as control for 72 h in HK-2 cells. (B) Quantitative analysis of the immunofluorescence staining LaminB1 showed a significant difference between the control group and BSA group (10 mg/mL). (C) LaminB1 mRNA level was detected by qRT-PCR. The expression of LaminB1 is downregulated after BSA treatment for 72 h in HK-2 cells. (D) The protein expression of γ-H2AX was determined by western blot analysis. (E) Quantitative analysis of the western blot showed that after HK-2 cells were treated with BSA for 72 h, the γ-H2AX expression was increased compared with the control group. *$P < 0.05$, and **$P < 0.01$ vs control.
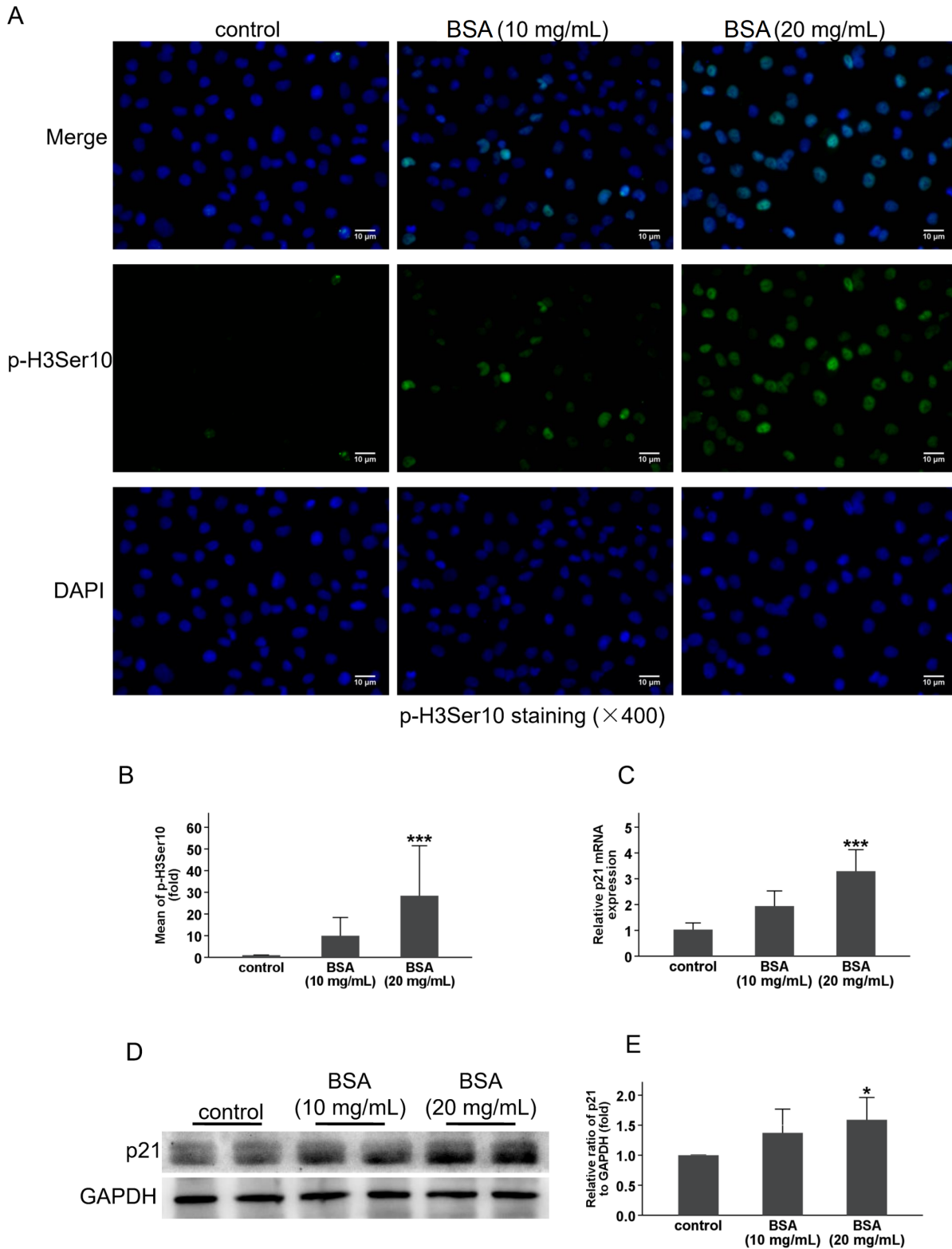
Figure 3. BSA induced the G2/M phase arrest and p21 expression HK-2 cells were treated with BSA or normal medium as control for 72 h. (A) Immunofluorescence staining showed a concentration-dependent increase in p-H3Ser10. (B) Quantitative analysis of immunofluorescence staining of p-H3Ser10 showed a significant difference between the BSA (20 mg/mL) group and the control group. (C) p21 mRNA level was detected by qRT-PCR. The expression of p21 was upregulated and showed a significant difference with the control group after BSA (20 mg/mL) treatment. (D) The protein expression of p21 was determined by western blot analysis. (E) Quantitative analysis showed the protein expression of p21 in BSA group was increased compared with the control group. $*P < 0.05$, and $***P < 0.001$ vs control.
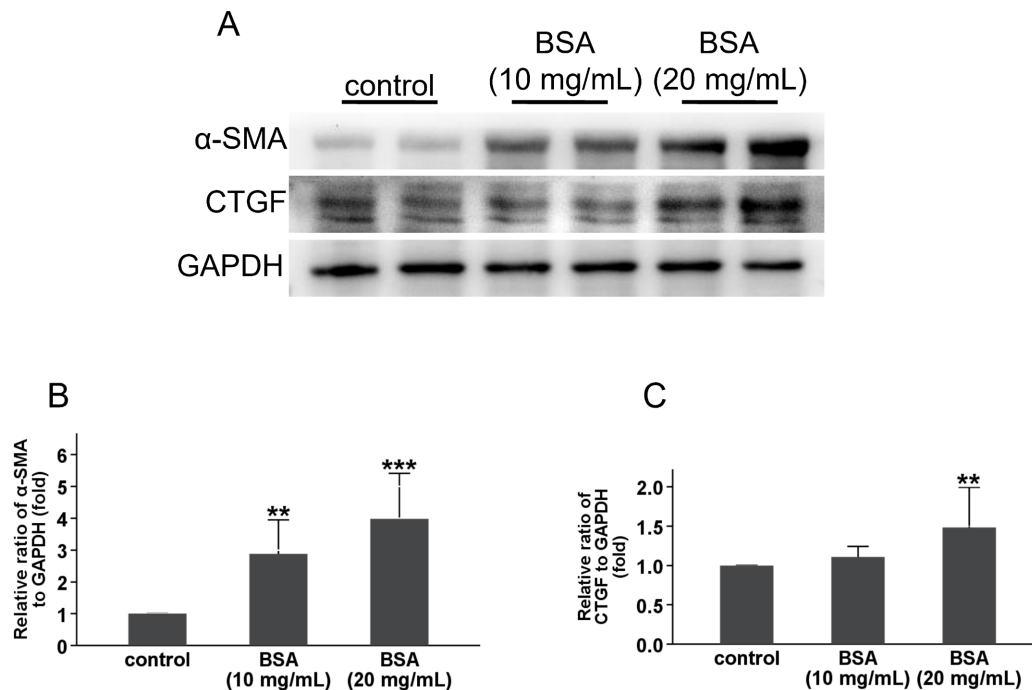
Figure 4. BSA stimulated the profibrotic factors in HK-2 cells HK-2 cells were cultured in different concentrations of BSA for 72 h. (A) The protein expressions of CTGF and α-SMA were determined by western blot analysis. (B,C) HK-2 cells were treated with BSA for 72 h, quantitative analysis showed that the protein expressions of CTGF and α-SMA were increased compared with the control group. **$P < 0.01$, and ***$P < 0.001$ vs control.

compared to those in renal TECs without Megalin receptor knock-out. These studies did not explicitly show that inhibiting albumin reuptake improved cellular senescence, but inflammatory factors, oxidative stress, and apoptosis, which are closely related to senescent phenotypes, were indeed improved. On the other hand, Klotho is a well-known anti-aging marker. Beatriz et al. [45] found that Klotho was decreased in the urine of patients with severe proteinuria. Experimental proteinuria nephropathy is associated with a decline in Klotho in animal models, and albumin directly reduces the Klotho expression in cultured renal tubular cells in vitro. These results suggest that albumin may induce the senescence of renal TECs.

To test our hypothesis, cultured tubular cells exposed to BSA were used as surrogates for the in vivo exposure of tubular cells to albumin in proteinuric nephropathies [46]. First, the presence of senescent cells should be identified after the intervention of HK-2 cells with different BSA concentrations. Due to different cell types, tissues, species and other factors, there is no single marker for senescent cells. Therefore, it is recommended to combine various senescence markers with multiple detection methods to detect senescent cells at present [47]. After HK-2 cells were treated with BSA, the decrease in cell density could be seen under a microscope, indicating the decrease in cell proliferation ability. LaminB1 was significantly reduced, but the activities of SA-β-gal and common SASP components, such as IL-1α, IL-6, and IL-8, were increased. Cells arrested at the G2/M phase suggested that a normal cell cycle progression was disrupted, and the elevated γ-H2AX expression indicated that there was DNA damage (Figures 1–3). Therefore, we believe that albumin can induce premature senescence in renal

TECs in vitro.

Cell cycle arrest is one of the common features of senescent cells [47]. Previous studies revealed that TECs also have inadequate cell cycle progression in chronic kidney disease. Injured renal TECs are mainly blocked at the G2/M phase [16,25,27]. Therefore, we aimed to explore whether albuminuria-induced renal injury is caused by TECs blocked at the G2/M phase due to premature senescence. Based on in vitro studies, BSA could induce premature senescence in HK-2 cells, and we further confirmed that the number of HK-2 cells induced by BSA was increased significantly at the G2/M phase, as revealed by p-H3Ser10 staining (Figure 3A,B), which is a hallmark feature of cells arrested in the G2/M stage [16]. Current studies suggest that cell arrest at the G2/M phase can be considered as a predictive feature of renal fibrosis progression [16,48,49]. Meanwhile, previous studies showed that albuminuria promotes renal interstitial inflammation and fibrosis [5,6]. The major factors investigated here and shown to be upregulated in BSA-induced HK-2 cells are CTGF and α-SMA (Figure 4), which have been proven to play key roles in the development of fibrosis.

Cell cycle progression is mediated by the activation of CDKs. The p21, a CDK inhibitor, plays multiple roles in the regulation of both cell cycle and cellular senescence [50–52]. It was reported that p21-deficient mice could avoid liver fibrosis because of the elimination of senescent liver stellate cells [53]. In DKD animal models, p21 expression was increased with the upregulation of SA-β-gal activity in TECs [21]. Furthermore, senescence induced by high glucose level was inhibited when p21 was knocked down in cultured human proximal tubular cells, indicating that the senescence of renal TECs is related to the p21-dependent pathway [20]. Therefore, we spec-
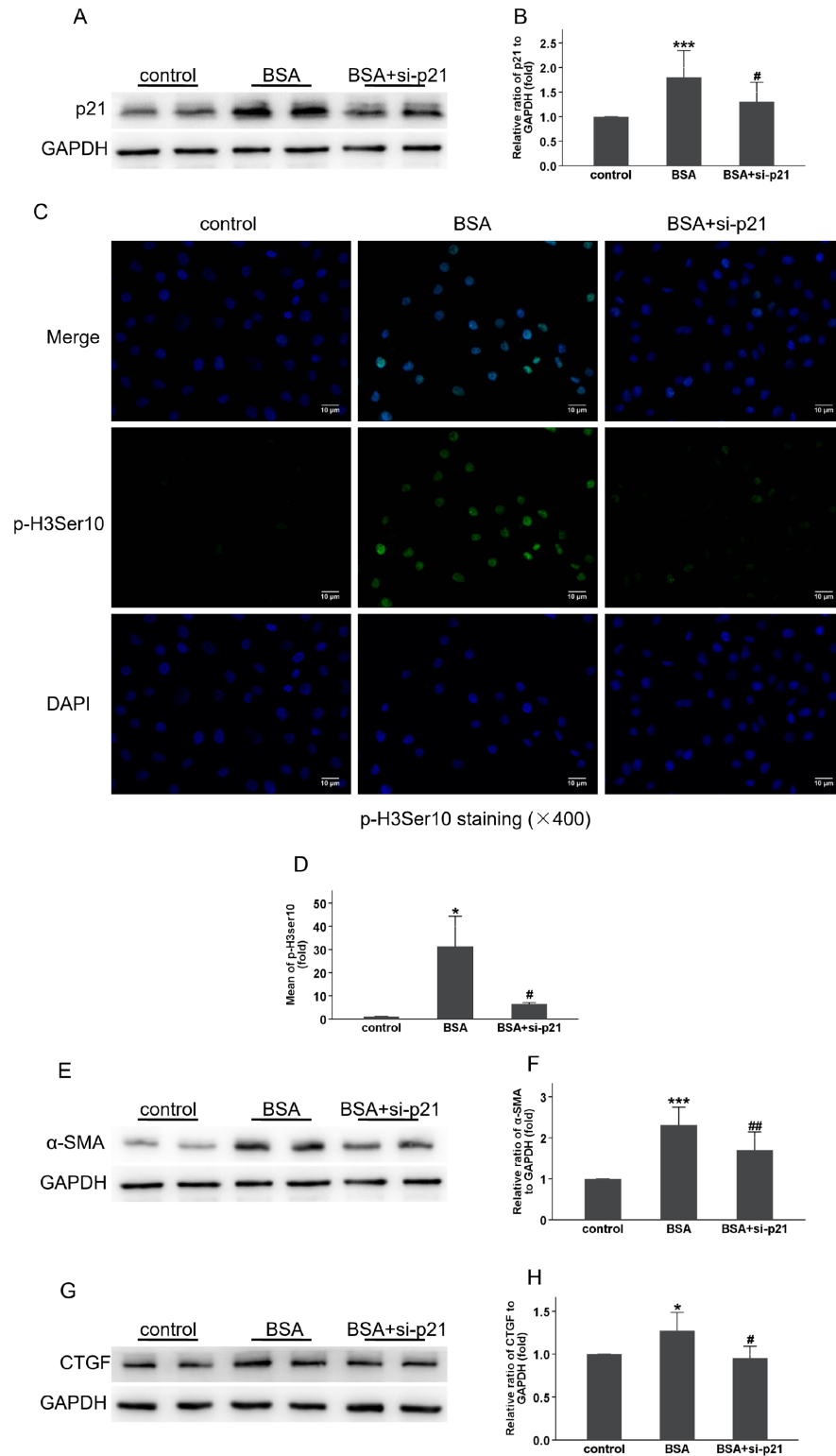
Figure 5. Inhibition of p21 prevented the G2/M arrest and fibrogenesis HK-2 cells were cultured in 20 mg/mL BSA and/or siRNA p21 for 72 h. (A) The protein expression of p21 was determined by western blot analysis. (B) Quantification p21 expression in HK-2 cells treated as indicated. (C) Immunofluorescence staining showed that p-H3Ser10 was decreased in HK-2 cells transfected with si-p21. (D) Quantitative analysis of immunofluorescence staining of p-H3Ser10 showed significant difference between the BSA + si-p21 group and the BSA (20 mg/mL) group. (E,G) The protein expressions of CTGF and α-SMA were determined by western blot analysis. (F,H) HK-2 cells were treated with BSA + si-p21 for 72 h, the expressions of both CTGF and α-SMA were decreased compared with the BSA (20 mg/mL) group. $*P < 0.05$, and $***P < 0.001$ vs control; $^{\#}P < 0.05$, and $^{\#\#}P < 0.01$ vs BSA.
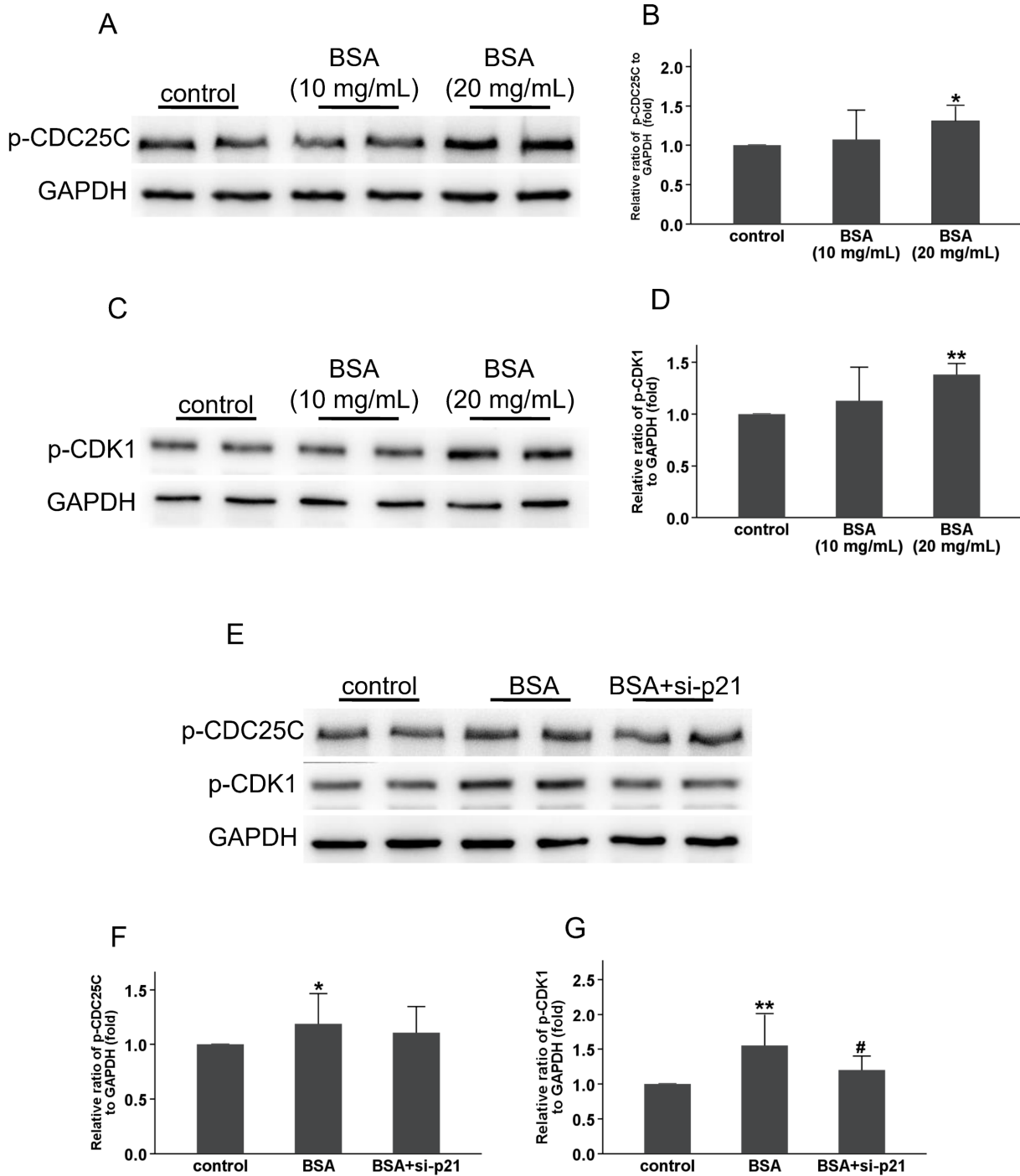
Figure 6. BSA caused G2/M phase arrest by activating the CDC25C/CDK1 pathway (A–D) The expressions of p-CDC25C and p-CDK1 in HK-2 cells treated with various concentrations of BSA were measured by western blot analysis. In the BSA (20 mg/mL) group, the phosphorylation of both CDC25C and CDK1 was upregulated compared with those in the control group with significant difference. (E–G) After HK-2 cells were treated with 20 mg/mL BSA combined si-p21 for 72 h, the protein expressions of p-CDC25C and p-CDK1 were determined by western blot analysis. The levels of both p-CDC25C and p-CDK1 were decreased compared with those of the BSA alone group. $*P < 0.05$, and $**P < 0.01$ vs control; $^{#}P < 0.05$ vs BSA.

ulate that p21 may also be involved in the BSA-induced premature senescence of HK-2 cells. As shown in Figure 3C–E, mRNA and protein expression of p21 was increased gradually with the increase

in BSA concentration, and the inhibition of p21 could alleviate BSA-induced HK-2 cells G2/M phase arrest (Figure 5C,D). Since the G2/M phase arrest was alleviated, further experiments showed that the

generation of CTGF and α-SMA could be significantly reduced by knockdown of p21 (Figure 5E–H). These results suggest that the premature senescence induced by BSA stimulates increased expression of p21, thereby promoting fibrosis by regulating the G2/M phase.

We further explored how p21 affects the G2/M phase arrest of BSA-induced HK-2 cells. The G2/M phase transition is directly regulated by the CDK1-cyclinB1 complexes. CDK1 dephosphorylation is required for the activation of CDK1-cyclin B1 complexes [54]. During G2/M arrest, CDK1-cyclinB1 complexes are kept in an inactive state by phosphorylation at the conserved tyrosine 15 residue of CDK1 [55]. However, CDK1 dephosphorylation is regulated by activated CDC25C, and the CDC25C activity is achieved by downregulating Ser216 phosphorylation [56]. Thus, the reduced activity of CDC25C and the subsequent increase in CDK1 phosphorylation are the hallmarks of cell cycle arrest at the G2/M phase [29]. With the increase in BSA concentration, p-CDC25C-Ser216 and p-CDK1-Tyr15 were found to be increased gradually in our study (Figure 6A–D). These results suggest that BSA halts the cell cycle at the G2/M phase in a concentration-dependent manner. Next, whether p21 affects the cell cycle progression through the CDC25C/CDK1 pathway is worth exploring. We found that CDC25C and CDK1 phosphorylation can be inhibited by inhibiting the increase in p21 expression (Figure 6E–G). These results suggest that p21 influences the state of CDK1-cyclinB1 complexes through the CDC25C/CDK1 pathway to affect the G2/M phase progression.

In summary, we demonstrate here that BSA induces a series of senescent phenotypes. Finally, these changes lead to premature senescence to activate p21 expression in HK-2 cells, and p21 regulates the cell cycle arrest at the G2/M phase through the CDC25C/CDK1 pathway, which eventually leads to an increase in fibrosis. This study improves our understanding on BSA-induced premature senescence of TECs, which is associated with fibrosis. Moreover, delaying the senescence of renal TECs may be an important means to improve the renal interstitial fibrosis induced by albuminuria.

Funding

Conflict of Interest

The authors declare that they have no conflict of interest.

References

1. Dabelea D, Stafford JM, Mayer-Davis EJ, D'Agostino Jr R, Dolan L, Imperatore G, Linder B, et al. Association of type 1 diabetes vs type 2 diabetes diagnosed during childhood and adolescence with complications during teenage years and young adulthood. JAMA 2017, 317: 825–835

2. Berhane AM, Weil EJ, Knowler WC, Nelson RG, Hanson RL. Albuminuria and estimated glomerular filtration rate as predictors of diabetic end-stage renal disease and death. Clin J Am Soc Nephrol 2011, 6: 2444–2451

3. Andrassy KM. Comments on 'KDIGO 2012 clinical practice guideline for the evaluation and management of chronic kidney disease'. Kidney Int 2013, 84: 622–623

4. Liu Y. Cellular and molecular mechanisms of renal fibrosis. Nat Rev Nephrol 2011, 7: 684–696

5. Eddy AA, Giachelli CM, McCulloch L, Liu E. Renal expression of genes that promote interstitial inflammation and fibrosis in rats with protein-overload proteinuria. Kidney Int 1995, 47: 1546–1557

6. Eddy AA, Kim H, López-Guisa J, Oda T, Soloway PD, McCulloch L, Liu E, et al. Interstitial fibrosis in mice with overload proteinuria: deficiency of TIMP-1 is not protective. Kidney Int 2000, 58: 618–628

7. Gansevoort RT, Navis GJ, Wapstra FH, de Jong PE, de Zeeuw D. Proteinuria and progression of renal disease. Curr Opin Nephrol Hypertension 1997, 6: 133–140

8. Gewin LS. Renal fibrosis: Primacy of the proximal tubule. Matrix Biol 2018, 68-69: 248–262

9. Liu BC, Tang TT, Lv LL, Lan HY. Renal tubule injury: a driving force toward chronic kidney disease. Kidney Int 2018, 93: 568–579

10. Ferenbach DA, Bonventre JV. Mechanisms of maladaptive repair after AKI leading to accelerated kidney ageing and CKD. Nat Rev Nephrol 2015, 11: 264–276

11. Bonventre JV. Primary proximal tubule injury leads to epithelial cell cycle arrest, fibrosis, vascular rarefaction, and glomerulosclerosis. Kidney Int Supplements 2014, 4: 39–44

12. Andrade L, Rodrigues CE, Gomes SA, Noronha IL. Acute kidney injury as a condition of renal senescence. Cell TransPlant 2018, 27: 739–753

13. Muñoz-Espín D, Serrano M. Cellular senescence: from physiology to pathology. Nat Rev Mol Cell Biol 2014, 15: 482–496

14. Li Q, Chen C, Chen X, Han M, Li J. Dexmedetomidine attenuates renal fibrosis via α2-adrenergic receptor-dependent inhibition of cellular senescence after renal ischemia/reperfusion. Life Sci 2018, 207: 1–8

15. Xiong Y, Zhou L. The signaling of cellular senescence in diabetic nephropathy. Oxid Med Cell Longev 2019, 2019: 1–16

16. Yang L, Besschetnova TY, Brooks CR, Shah JV, Bonventre JV. Epithelial cell cycle arrest in G2/M mediates kidney fibrosis after injury. Nat Med 2010, 16: 535–543

17. Lai L, Shin GY, Qiu H. The role of cell cycle regulators in cell survival—dual functions of cyclin-dependent kinase 20 and p21cip1/waf1. Int J Mol Sci 2020, 21: 8504

18. Fischer M, Quaas M, Steiner L, Engeland K. The p53-p21-DREAM-CDE/CHR pathway regulates G$_2$/M cell cycle genes. Nucleic Acids Res 2016, 44: 164–174

19. Hernandez-Segura A, Nehme J, Demaria M. Hallmarks of cellular senescence. Trends Cell Biol 2018, 28: 436–453

20. Kitada K, Nakano D, Ohsaki H, Hitomi H, Minamino T, Yatabe J, Felder RA, et al. Hyperglycemia causes cellular senescence via a SGLT2- and p21-dependent pathway in proximal tubules in the early stage of diabetic nephropathy. J Diabetes its Complications 2014, 28: 604–611

21. Satriano J, Mansoury H, Deng A, Sharma K, Vallon V, Blantz RC, Thomson SC. Transition of kidney tubule cells to a senescent phenotype in early experimental diabetes. Am J Physiol-Cell Physiol 2010, 299: C374–C380

22. Hernandez-Segura A, de Jong TV, Melov S, Guryev V, Campisi J, Demaria M. Unmasking transcriptional heterogeneity in senescent cells. Curr Biol 2017, 27: 2652–2660.e4

23. Sadaie M, Salama R, Carroll T, Tomimatsu K, Chandra T, Young ARJ, Narita M, et al. Redistribution of the Lamin B1 genomic binding profile affects rearrangement of heterochromatic domains and SAHF formation during senescence. Genes Dev 2013, 27: 1800–1808

24. Siddiqui MS, François M, Fenech MF, Leifert WR. Persistent γH2AX: A promising molecular marker of DNA damage and aging. Mutat Res Rev Mutat Res 2015, 766: 1–19

25. Canaud G, Bonventre JV. Cell cycle arrest and the evolution of chronic kidney disease from acute kidney injury. Nephrol Dial Transplant 2015, 30: 575–583

26. Witzgall R, Brown D, Schwarz C, Bonventre JV. Localization of proliferating cell nuclear antigen, vimentin, c-Fos, and clusterin in the post-

ischemic kidney. Evidence for a heterogenous genetic response among nephron segments, and a large pool of mitotically active and dedifferentiated cells. *J Clin Invest* 1994, 93: 2175–2188

27. Duffield JS, Park KM, Hsiao LL, Kelley VR, Scadden DT, Ichimura T, Bonventre JV. Restoration of tubular epithelial cells during repair of the postischemic kidney occurs independently of bone marrow-derived stem cells. *J Clin Invest* 2005, 115: 1743–1755

28. Karimian A, Ahmadi Y, Yousefi B. Multiple functions of p21 in cell cycle, apoptosis and transcriptional regulation after DNA damage. *DNA Repair* 2016, 42: 63–71

29. Wang J, Chang L, Lai X, Li X, Wang Z, Huang Z, Huang J, *et al.* Tetrandrine enhances radiosensitivity through the CDC25C/CDK1/cyclin B1 pathway in nasopharyngeal carcinoma cells. *Cell Cycle* 2018, 17: 671–680

30. Bell S, Fletcher EH, Brady I, Looker HC, Levin D, Joss N, Traynor JP, *et al.* End-stage renal disease and survival in people with diabetes: a national database linkage study. *QJM* 2015, 108: 127–134

31. Kato M, Natarajan R. Diabetic nephropathy—emerging epigenetic mechanisms. *Nat Rev Nephrol* 2014, 10: 517–530

32. Heerspink HJL, Parving HH, Andress DL, Bakris G, Correa-Rotter R, Hou FF, Kitzman DW, *et al.* Atrasentan and renal events in patients with type 2 diabetes and chronic kidney disease (SONAR): a double-blind, randomised, placebo-controlled trial. *Lancet* 2019, 393: 1937–1947

33. Gross JL, de Azevedo MJ, Silveiro SP, Canani LH, Caramori ML, Zelmanovitz T. Diabetic nephropathy: diagnosis, prevention, and treatment. *Diabetes Care* 2005, 28: 164–176

34. Allouch S, Munusamy S. Metformin attenuates albumin-induced alterations in renal tubular cells *in vitro*. *J Cell Physiol* 2017, 232: 3652–3663

35. Hu J, Wang W, Zhang F, Li PL, Boini KM, Yi F, Li N. Hypoxia inducible factor-1α mediates the profibrotic effect of albumin in renal tubular cells. *Sci Rep* 2017, 7: 15878

36. Jheng HF, Tsai PJ, Chuang YL, Sheng YT, Tai TA, Chen WC, Chou CK, *et al.* Albumin stimulates renal tubular inflammation through a HSP70-TLR4 axis in early diabetic nephropathy. *Dis Model Mech* 2015

37. Nishi Y, Satoh M, Nagasu H, Kadoya H, Ihoriya C, Kidokoro K, Sasaki T, *et al.* Selective estrogen receptor modulation attenuates proteinuria-induced renal tubular damage by modulating mitochondrial oxidative status. *Kidney Int* 2013, 83: 662–673

38. Wu X, He Y, Jing Y, Li K, Zhang J. Albumin overload induces apoptosis in renal tubular epithelial cells through a chop-dependent pathway. *OMICS-J Integrative Biol* 2010, 14: 61–73

39. Thomas MC, Burns WC, Cooper ME. Tubular changes in early diabetic nephropathy. *Adv Chronic Kidney Dis* 2005, 12: 177–186

40. Valentijn FA, Falke LL, Nguyen TQ, Goldschmeding R. Cellular senescence in the aging and diseased kidney. *J Cell Commun Signal* 2018, 12: 69–82

41. Verzola D, Gandolfo MT, Gaetani G, Ferraris A, Mangerini R, Ferrario F, Villaggio B, *et al.* Accelerated senescence in the kidneys of patients with type 2 diabetic nephropathy. *Am J Physiol-Renal Physiol* 2008, 295: F1563–F1573

42. Nolin AC, Mulhern RM, Panchenko MV, Pisarek-Horowitz A, Wang Z, Shirihai O, Borkan SC, *et al.* Proteinuria causes dysfunctional autophagy in the proximal tubule. *Am J Physiol-Renal Physiol* 2016, 311: F1271–F1279

43. Liu D, Wen Y, Tang TT, Lv LL, Tang RN, Liu H, Ma KL, *et al.* Megalin/Cubulin-lysosome-mediated albumin reabsorption is involved in the tubular cell activation of nlrp3 inflammasome and tubulointerstitial inflammation. *J Biol Chem* 2015, 290: 18018–18028

44. Motoyoshi Y, Matsusaka T, Saito A, Pastan I, Willnow TE, Mizutani S, Ichikawa I. Megalin contributes to the early injury of proximal tubule cells during nonselective proteinuria. *Kidney Int* 2008, 74: 1262–1269

45. Fernandez-Fernandez B, Izquierdo MC, Valiño-Rivas L, Nastou D, Sanz AB, Ortiz A, Sanchez-Niño MD. Albumin downregulates Klotho in tubular cells. *Nephrol Dial Transplant* 2018, 33: 1712–1722

46. Sanchez-Niño MD, Fernandez-Fernandez B, Perez-Gomez MV, Poveda J, Sanz AB, Cannata-Ortiz P, Ruiz-Ortega M, *et al.* Albumin-induced apoptosis of tubular cells is modulated by BASP1. *Cell Death Dis* 2015, 6: e1644

47. Gorgoulis V, Adams PD, Alimonti A, Bennett DC, Bischof O, Bishop C, Campisi J, *et al.* Cellular senescence: defining a path forward. *Cell* 2019, 179: 813–827

48. Lovisa S, LeBleu VS, Tampe B, Sugimoto H, Vadnagara K, Carstens JL, Wu CC, *et al.* Epithelial-to-mesenchymal transition induces cell cycle arrest and parenchymal damage in renal fibrosis. *Nat Med* 2015, 21: 998–1009

49. Zhao H, Jiang N, Han Y, Yang M, Gao P, Xiong X, Xiong S, *et al.* Aristolochic acid induces renal fibrosis by arresting proximal tubular cells in G2/M phase mediated by HIF-1α. *FASEB J* 2020, 34: 12599–12614

50. Child ES, Mann DJ. The intricacies of p21 phosphorylation: protein/protein interactions, subcellular localization and stability. *Cell Cycle* 2006, 5: 1313–1319

51. Jung YS, Qian Y, Chen X. Examination of the expanding pathways for the regulation of p21 expression and activity. *Cell Signalling* 2010, 22: 1003–1012

52. Gire V, Dulic V. Senescence from G2 arrest, revisited. *Cell Cycle* 2015, 14: 297–304

53. Yosef R, Pilpel N, Papismadov N, Gal H, Ovadya Y, Vadai E, Miller S, *et al.* p21 maintains senescent cell viability under persistent DNA damage response by restraining JNK and caspase signaling. *EMBO J* 2017, 36: 2280–2295

54. Smits VAJ, Klompmaker R, Vallenius T, Rijksen G, Mäkelä TP, Medema RH. p21 inhibits Thr161 phosphorylation of Cdc2 to enforce the G2 DNA damage checkpoint. *J Biol Chem* 2000, 275: 30638–30643

55. Fisher D, Krasinska L, Coudreuse D, Novák B. Phosphorylation network dynamics in the control of cell cycle transitions. *J Cell Sci* 2012, 125: 4703–4711

56. Nigg EA. Mitotic kinases as regulators of cell division and its checkpoints. *Nat Rev Mol Cell Biol* 2001, 2: 21–32